

Stable embedded solitons

Jianke Yang

Department of Mathematics and Statistics, University of Vermont, Burlington, VT 05401, USA

Stable embedded solitons are discovered in the generalized third-order nonlinear Schrödinger equation. When this equation can be reduced to a perturbed complex modified KdV equation, we developed a soliton perturbation theory which shows that a continuous family of sech-shaped embedded solitons exist and are nonlinearly *stable*. These analytical results are confirmed by our numerical simulations. These results establish that, contrary to previous beliefs, embedded solitons can be robust despite being in resonance with the linear spectrum. [PACS: 42.65.Tg, 05.45.Yv.]

Pulse propagation in optical fibers attracts a lot of attention these days. Pico-second pulses are well described by the nonlinear Schrödinger (NLS) equation which accounts for the second-order dispersion and self-phase modulation. But for femtosecond pulses, other physical effects such as the third-order dispersion and self-steepening become non-negligible. The physical model which incorporates these additional effects is [1,2]

$$i[\psi_z + \beta|\psi|^2\psi_\tau + \mu(|\psi|^2)_\tau\psi] + \frac{1}{2}\psi_{\tau\tau} + |\psi|^2\psi + i\psi_{\tau\tau\tau} = 0. \quad (1)$$

Here ψ is the envelope of the electric field, z is the distance, τ is the retarded time, β and μ are the self-steepening coefficients [1]. All quantities have been normalized. For optical pulses, $\beta = \mu$ [1,2]. In this paper, we allow β and μ to be different for the sake of mathematical analysis. The Raman effect, which is dissipative in nature, is also non-negligible [1,2]. It is not included in the model (1) because we want to focus our attention on the other physical effects in this paper.

The third-order dispersion term in Eq. (1) is significant because it qualitatively changes the linear dispersion relation of Eq. (1). Its effect on the NLS soliton is to generate continuous-wave radiation and causes the soliton to decay [1–5]. However, solitary waves of Eq. (1) which are embedded inside the linear spectrum do exist in certain parameter regimes [6–9], and such waves are called embedded solitons [10,11]. To see why a solitary wave of Eq. (1) has to be an embedded soliton, we substitute solitary waves of the form $\Psi(\tau - Vz)e^{i\lambda z}$ into (1), where velocity V and frequency λ are constants. We readily find that for any frequency λ , the linear equation for Ψ allows oscillatory solutions. Thus, all λ lies in the continuous spectrum of Eq. (1), hence the solitary wave must be an embedded soliton. Stability of these embedded solitons is clearly an important issue. Previous analytical studies have shown that if embedded solitons are isolated in a conservative system, they are at most semi-stable, i.e., the perturbed soliton persists or decays depending on whether the initial energy is higher or lower than that of the embedded soliton [10,12,13]. A physical explanation for it is as follows [10]. If the initial state has energy higher than the embedded soliton, it just

sheds extra energy through tail radiation and asymptotically approaches this embedded soliton; but if the initial state has lower energy than the embedded soliton, the energy loss (through radiation) drives the solution away from the embedded soliton, resulting in instability. However, embedded solitons in Eq. (1) are *not isolated*: they exist as a continuous family, parameterized by their energy [8,9]. Thus, the above physical argument for semi-stability does not apply. Numerical results suggest that the families of double-hump embedded solitons in Eq. (1) are still semi-stable [9], but the family of single-hump embedded solitons are fully stable [14].

In this paper, we show that single-hump embedded solitons in Eq. (1) are fully stable when $|\beta - 6| \ll 1$ and $|\mu| \ll 1$. To our knowledge, this is the first time *stable* embedded solitons are rigorously established in the literature. This result indicates that embedded solitons can be as robust as conventional (non-embedded) solitons, contrary to the previous belief. The method we will use is to develop a soliton perturbation theory for the (integrable) complex modified KdV (CMKdV) equation, supplemented by numerical simulations.

We first employ the variable transformation

$$\psi = e^{\frac{1}{6}i(\tau - \frac{1}{18}z)} \sqrt{\frac{6}{\beta}} u(z, \xi), \quad \xi \equiv \tau - \frac{1}{12}z, \quad (2)$$

upon which Eq. (1) becomes

$$u_z + u_{\xi\xi\xi} + 6|u|^2u_\xi = i\alpha|u|^2u - \gamma(|u|^2)_\xi u, \quad (3)$$

where $\alpha = (6 - \beta)/\beta$, and $\gamma = 6\mu/\beta$. If $\alpha = \gamma = 0$, the above equation is the CMKdV equation which is completely integrable by the inverse scattering method [15]. It admits sech-shaped soliton solutions whose amplitudes and velocities are free parameters (see below). In this paper, we consider the case $|\alpha|, |\gamma| \ll 1$, i.e., $|\beta - 6| \ll 1$ and $|\mu| \ll 1$. In this limit, soliton evolution in the perturbed CMKdV equation (3) can be studied by a soliton perturbation theory. For this purpose, we denote $\alpha = \epsilon\alpha_0, \gamma = \epsilon\gamma_0$, where $|\epsilon| \ll 1$. When $\epsilon = 0$, Eq. (3) has the following soliton solutions

$$u_0(z, \xi) = U_0(\theta)e^{i\lambda z}, \quad \theta \equiv \xi - Vz, \quad (4)$$

where

$$U_0(\theta) = r \operatorname{sech} r \theta e^{ik\theta}, \quad V = r^2 - 3k^2, \quad \lambda = -2k(r^2 + k^2). \quad (5)$$

Here amplitude r and frequency k are free parameters. When $0 \neq |\epsilon| \ll 1$, these solitons will deform due to perturbations on the right hand side of Eq. (3), and their amplitudes and frequencies will undergo slow evolution with respect to z . Below, we use the soliton perturbation theory to derive this evolution.

First, we write the solution in the form

$$u(z, \xi) = e^{i \int_0^z \lambda dz} U(z, \theta), \quad \theta = \xi - \int_0^z V dz. \quad (6)$$

Substituting this form into (3), we find the equation for $U(z, \theta)$ as

$$U_z + i\lambda U - V U_\theta + U_{\theta\theta\theta} + 6|U|^2 U_\theta = \epsilon F(U), \quad (7)$$

where

$$F(U) = [i\alpha_0 |U|^2 - \gamma_0 (|U|^2)_\theta] U. \quad (8)$$

Next, we expand the solution U into a perturbation series

$$U(z, \theta) = U_0(\theta) + \epsilon U_1(z, \theta) + \epsilon^2 U_2(z, \theta) + \dots, \quad (9)$$

where U_0 is given in (5). When this series is substituted into Eq. (7), at order 1, the equation is satisfied automatically. At order ϵ , we obtain the linear inhomogeneous equation for U_1 as

$$\left(\frac{\partial}{\partial z} + \mathcal{L} \right) \begin{pmatrix} U_1 \\ U_1^* \end{pmatrix} = \begin{pmatrix} F(U_0) \\ F^*(U_0) \end{pmatrix}, \quad (10)$$

where \mathcal{L} is the linearization operator of Eq. (7), and superscript “*” denotes the complex conjugation. At initial distance $z = 0$, $U_1 = 0$; when $z \gg 1$, U_1 approaches a steady state with continuous-wave tails at infinity. Generation of continuous-wave tails is a distinctive feature of embedded solitons under perturbations [10]. These tails have the form $h e^{-2ik\theta}$, where h is the tail amplitude. Due to the Sommerfeld radiation condition, these tails can only appear at $\theta \ll -1$, not at $\theta \gg 1$. In other words,

$$\lim_{z \rightarrow \infty, \theta \ll -1} U_1 = h e^{-2ik\theta}, \quad \lim_{z \rightarrow \infty, \theta \gg 1} U_1 = 0. \quad (11)$$

One of the key steps in the soliton perturbation theory is to determine the amplitude h of continuous-wave tails in U_1 . This can be done by solving Eq. (10) directly, starting with the zero initial condition [13]. The way to do it is to expand the solution into the complete set of eigenfunctions for the linearization operator \mathcal{L} , which are just the squared eigenstates of the Zakharov-Shabat system with the soliton potential [16]. This we have done. But a much simpler way to derive h is to just consider the steady-state solution U_1 . This allows us to drop the z derivative in Eq. (10), and use only solvability conditions to obtain h . This idea has been used before [12].

To pursue this latter approach, we need the bounded eigenfunctions of the adjoint linearization operator \mathcal{L}^A with zero eigenvalue. Here the inner product used to define an adjoint operator is

$$\langle f(\theta), g(\theta) \rangle = \int_{-\infty}^{\infty} f(\theta)^T g(\theta) d\theta, \quad (12)$$

where the superscript “ T ” represents the transpose of a vector. Under this inner product, the adjoint operator \mathcal{L}^A can be readily obtained. Eigenfunctions of \mathcal{L}^A are simply a different set of squared Zakharov-Shabat eigenstates [16]. With this in mind, we can easily show that \mathcal{L}^A has four bounded eigenfunctions for zero eigenvalue — two localized and two non-localized. The localized (discrete) eigenfunctions are

$$\Phi_1 = \begin{bmatrix} U_{0\theta}^* \\ -U_{0\theta} \end{bmatrix}, \quad \Phi_2 = \begin{bmatrix} U_0^* \\ U_0 \end{bmatrix}. \quad (13)$$

They are associated with the translational and phase invariances of solitons in the CMKdV equation. The non-localized (continuous) eigenfunctions are

$$\Phi_3 = \begin{bmatrix} r^2 \operatorname{sech}^2 r \theta e^{-4ik\theta} \\ (r \tanh r \theta + 3ik)^2 e^{-2ik\theta} \end{bmatrix}, \quad (14)$$

$$\Phi_4 = \begin{bmatrix} (r \tanh r \theta - 3ik)^2 e^{2ik\theta} \\ r^2 \operatorname{sech}^2 r \theta e^{4ik\theta} \end{bmatrix}. \quad (15)$$

Now we take the inner product between Eq. (10) (with no z derivative) and each of the above four eigenfunctions. In view of the asymptotics (11), we see that the first two inner-product equations are simply

$$\left\langle \Phi_1, \begin{pmatrix} F(U_0) \\ F^*(U_0) \end{pmatrix} \right\rangle = \left\langle \Phi_2, \begin{pmatrix} F(U_0) \\ F^*(U_0) \end{pmatrix} \right\rangle = 0, \quad (16)$$

which are satisfied automatically when the form (8) for $F(U)$ is utilized. The last two inner-product equations are equivalent. After simple calculations, these equations give a formula for the amplitude h as

$$h = -\frac{1}{4} i \pi (\alpha_0 + 2\gamma_0 k) \frac{r - 3ik}{r + 3ik} \operatorname{sech} \frac{3\pi k}{2r}. \quad (17)$$

When the tail amplitude h has been derived, we can proceed to order ϵ^2 . Again, by applying the solvability conditions for solution U_2 , the dynamical equations for soliton parameters r and k will be obtained (see [12] for an example). An alternative way to derive these dynamical equations, which is simpler and physically more insightful, is by using conservation laws [12]. In this latter way we will proceed.

Eq. (3) admits the following two conservation laws:

$$I_1 = \int_{-\infty}^{\infty} |u|^2 d\xi, \quad (18)$$

$$I_2 = \int_{-\infty}^{\infty} \left\{ \frac{1}{2} i \alpha (u_\xi u^* - u u_\xi^*) - \gamma |u_\xi|^2 + \gamma \left(1 + \frac{1}{3} \gamma\right) |u|^4 \right\} d\xi. \quad (19)$$

When Eq. (6) and the perturbation series (9) are substituted into these conservation laws and terms up to order ϵ^2 retained, the first conservation law becomes

$$\frac{d}{dz} \int_{-\infty}^{\infty} \left\{ |U_0|^2 + \epsilon (U_0 U_1^* + U_0^* U_1) + \epsilon^2 (U_0 U_2^* + U_0^* U_2) + \epsilon^2 |U_1|^2 \right\} = 0. \quad (20)$$

To proceed further, the following facts are noted: (i) $|U_0|^2$ changes slowly (on the distance scale $\epsilon^2 z$); (ii) the U_1 field is driven by the inhomogeneous term in Eq. (10) and quickly becomes stationary in the soliton (U_0) region; the U_2 field is similar; (iii) the U_1 field develops a continuous-wave tail of amplitude h on the left-hand-side of the soliton [see Eq. (11)]; this tail travels at its group velocity $v_g = -12k^2$; in the moving coordinate ξ , its relative velocity is $v_g - V = -(r^2 + 9k^2)$ [see Eq. (5)]. The fact (ii) means that the z derivatives of the integrals of the second and third terms in Eq. (20) are zero and can be dropped. The fact (iii) means that the z derivative of the integral of the last term in (20) is $\epsilon^2 (r^2 + 9k^2) |h|^2$. When these results and the U_0 formula (5) are utilized, the first conservation law (20) gives the dynamical equation for the soliton amplitude r . Similar calculations for the second conservation law produces the dynamical equation for the soliton frequency k . When the h formula (17) is substituted, and $(\epsilon \alpha_0, \epsilon \gamma_0)$ replaced by the physical parameters (α, γ) , the dynamical equations for r and k finally take the form

$$\frac{dr}{dz} = -\frac{1}{32} \pi^2 (\alpha + 2\gamma k)^2 (r^2 + 9k^2) \operatorname{sech}^2 \frac{3\pi k}{2r}, \quad (21)$$

$$\frac{dk}{dz} = \frac{1}{32r} \pi^2 (\alpha + 2\gamma k) [3\alpha k - \gamma (r^2 + 3k^2)] (r^2 + 9k^2) \operatorname{sech}^2 \frac{3\pi k}{2r}, \quad (22)$$

and they govern the soliton evolution under small perturbations $|\alpha|, |\gamma| \ll 1$ in Eq. (3). These two equations are the main analytical results of this paper.

Dynamical equations (21) and (22) admit a continuous family of fixed points:

$$k = -\frac{\alpha}{2\gamma}, \quad r \text{ is arbitrary.} \quad (23)$$

These fixed points correspond to a continuous family of embedded solitons (4) in the original wave equation (3). Their amplitudes r are arbitrary, while their speeds V depend on r according to Eq. (5). It is easy to check that these embedded solitons are precisely the ones reported in [8]. We have further determined the linear and nonlinear stabilities of these fixed points in equations (21) and (22), and found that they are all *stable*, both linearly and nonlinearly. This means that these sech-shaped embedded solitons in the perturbed CMKdV equation (3) are both linearly and nonlinearly *stable*, despite the fact

that such solitons reside inside the continuous spectrum of the wave system and are in resonance with the continuous waves. They mark a distinct contrast with isolated embedded solitons and the continuous family of double-hump embedded solitons in other physical systems, which were shown to be semi-stable [9,10,12,13].

The simplest way to demonstrate the linear and nonlinear stabilities of fixed points (23) is by drawing a phase portrait in the (r, k) plane. Such a phase portrait with $\alpha = -0.1$ and $\gamma = 0.1$ is shown in Fig. 1. At these parameter values, the fixed points are the $k = \frac{1}{2}$ line (dashed). Clearly, we see that these points are nonlinearly stable, and they attract a large region of initial parameters. At other α and γ values where $\alpha\gamma < 0$, the phase portraits are qualitatively similar. If $\alpha\gamma > 0$, the phase portrait is just the one of $\alpha\gamma < 0$ with k replaced by $-k$.

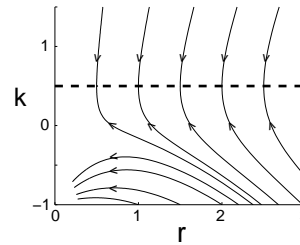


FIG. 1. Phase portrait of the dynamical system (21) and (22) for physical parameters $\alpha = -0.1$ and $\gamma = 0.1$.

Lastly, we confirm the above analytical results by direct numerical simulations of Eq. (3). Our numerical scheme is the pseudo-spectral method along the ξ direction, and the fourth-order Runge-Kutta method along the z direction. Damping boundary conditions have also been used to filter out the energy radiation emitted into the far field. A number of numerical simulations of Eq. (3), starting with the soliton solution (4) at $z = 0$, have been performed for various small α and γ values. Good agreement between the numerics and the analysis has been observed. In addition, as α and γ approach zero, the difference between the leading-order perturbation results [Eqs. (21) and (22)] and numerical values approaches zero, meaning that our perturbation theory is asymptotically accurate. For illustration purpose, we fix the physical parameters $\alpha = -0.1$ and $\gamma = 0.1$, and choose two sets of initial amplitude and frequency values, $(r_0, k_0) = (1.5, 1)$ and $(1.5, 0)$, which are on the opposite sides of the line of fixed points in Fig. 1. The simulation results are displayed in Fig. 2. For $(r_0, k_0) = (1.5, 1)$, the pulse evolution is plotted in Fig. 2(a). Due to perturbations in Eq. (3), the speed of the pulse slowly increases. Thus the pulse turns around and eventually approaches a steady positive speed. In Fig. 2(b), the field profiles at two distances are plotted. As predicted, a continuous-wave tail develops on the left of the embedded soliton. Note that the tail amplitude decreases with distance z ,

meaning that the embedded soliton is stabilizing [10]. A direct comparison between the numerics and the leading-order perturbation theory in the phase plane is shown in Fig. 2(d). We see that the numerical pulse frequency k indeed approaches the theoretical value $\frac{1}{2}$.

When $(r_0, k_0) = (1.5, 0)$, the numerical pulse evolution is displayed in Fig. 2(c). In this case, the soliton slows down under perturbations, contrary to the previous case. Examination of the radiation field indicates that the continuous-wave tails emitted to the left of the soliton are also lessening, indicating that the embedded soliton is stabilizing again as the theory predicts. Comparison in Fig. 2(d) between the numerics and the theory for this case also shows good agreement.

Physically, why are embedded solitons in Eq. (3) fully stable? There are two major reasons. First, these solitons exist as a continuous family. In other words, in the neighborhood of each embedded soliton, there are other embedded solitons nearby which have higher or lower energy. Thus when perturbed, an embedded soliton may always relax into an adjacent one, similar to the NLS-solitons. The second reason is that these embedded solitons are single-humped. Recall that double-humped embedded solitons in Eq. (1) also exist as a continuous family, but they are not stable [9]. This is not surprising, as the instability of multi-hump solitons is well documented in the literature. Embedded solitons in Eq. (3), however, are single-humped. Thus they could be fully stable as we have shown in this paper.

We note that for ultra-short pulses, $\beta = \mu$; while in this paper, $|\alpha|, |\gamma| \ll 1$, i.e., $|\beta - 6| \ll 1$ and $|\mu| \ll 1$. In the physical case $\beta = \mu$, a continuous family of single-hump embedded solitons also exists [8]. In addition, Gromov, et al's numerical computations show that a sech pulse tends to one or a few single-hump embedded solitons [14]. This numerical evidence, together with the above analytical results and physical arguments, strongly suggests that embedded solitons in this physical case are also stable. A rigorous proof of this full stability in this physical case can be provided by an elaborate internal-perturbation method [13], which we will pursue in the near future. It is also noted that for ultra-short pulses, the Raman effect is non-negligible. But since embedded solitons without the Raman effect are robust and stable, we can expect that the Raman effect on embedded solitons would be also a frequency downshift, similar to that on NLS solitons [1,2].

In summary, we have discovered fully-stable embedded solitons in a physical model relevant for ultra-short pulse propagation in optical fibers. This finding dispels previous skepticism about the observability of embedded solitons. We expect this work to have important impli-

cations to ultra-short pulse propagation. It would also stimulate further search for stable embedded solitons in other physical systems.

This work was supported in part by a NASA grant.

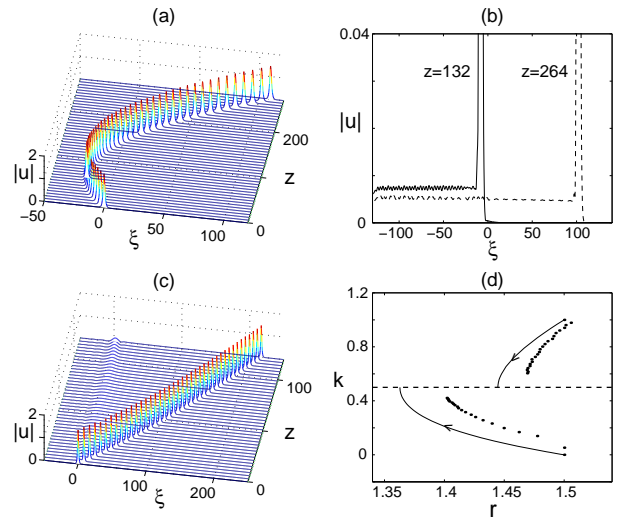


FIG. 2. Numerical evolution of initial solitons (4) with $r_0 = 1.5$, $k_0 = 1$ [in (a, b)] and 0 [in (c)] under perturbations of $\alpha = -0.1$ and $\gamma = 0.1$ in Eq. (3). In (d), numerical and analytical results are compared in the phase plane for both cases of $k_0 = 1$ and 0; solid lines: analytical; dots: numerical.

-
- [1] G.P. Agrawal, *Nonlinear Fiber Optics*. Academic Press, San Diego, 1989.
 - [2] A. Hasegawa and Y. Kodama, *Solitons in Optical Communications*. Clarendon Press, Oxford, 1995.
 - [3] P.K.A. Wai, et al., Phys. Rev. A 41, 426 (1990).
 - [4] R. Grimshaw, Stud. Appl. Math., 94, 257-270 (1995).
 - [5] Boyd, J.P., *Weakly nonlinear solitary waves and beyond-all-orders asymptotics*. Kluwer, Boston (1998).
 - [6] M. Klauder, et al., Phys. Rev. E 47, R3844 (1993).
 - [7] D.C. Calvo and T.R. Akylas, Physica D 101, 270 (1997).
 - [8] E.M. Gromov and V.V. Tyutin, Wave Motion 28, 13-24 (1998).
 - [9] J. Yang and T.R. Akylas, To appear in Stud. Appl. Math.
 - [10] J. Yang, B.A. Malomed, and D.J. Kaup, Phys. Rev. Lett. 83, 1958 (1999).
 - [11] A.R. Champneys, et al., Physica D 152, 340 (2001).
 - [12] J. Yang, Stud. Appl. Math. 106, 337 (2001).
 - [13] D.E. Pelinovsky, and J. Yang, Proc. Roy. Soc. Lond. A. 458, 1469-1497 (2002).
 - [14] E.M Gromov, L.V. Piskunova, V.V. Tyutin, Phys. Lett. A 256, 153 (1999).
 - [15] R. Hirota, J. Math. Phys. 14, 805 (1973).
 - [16] J. Yang, J. Math. Phys. 41, 6614 (2000).